ACS APPLIED MATERIALS & INTERFACES

Research Article

www.acsami.org

Negative Printing by Soft Lithography

Jason Kee Yang Ong,[†] David Moore,[†] Jennifer Kane,[†] and Ravi F. Saraf*[,†,‡]

[†]Department of Chemical and Biomolecular Engineering and [‡]Nebraska Center for Materials and Nanoscience, University of Nebraska—Lincoln, Lincoln, Nebraska 68588, United States

Supporting Information

ABSTRACT: In inkless microcontact printing (IμCP) by soft lithography, the poly(dimethylsiloxane) (PDMS) stamp transfers uncured polymer to a substrate corresponding to its pattern. The spontaneous diffusion of PDMS oligomers to the surface of the stamp that gives rise to this deleterious side effect has been leveraged to fabricate a variety of devices, such as organic thin film transistors, single-electron devices, and biomolecular chips. Here we report an anomalous observation on a partially cured PDMS stamp where the transfer of oligomers onto Au occurred on regions that were not in contact with the stamp, while the surface in contact with the stamp was pristine with no polymer. On the SiO_2 surface of the same chip, as expected, the transfer of PDMS occurred exclusively on regions in contact with the stamp. The printing on Au was quantified by a novel method where the submonolayer of PDMS transfer was measured by probing the local electrochemical passivation of the Au. The local transfer of polymer on SiO_2 (and also Au) was measured by selective deposition of Au nanoparticle necklaces that exclusively deposited on PDMS at submonolayer sensitivity. It was discovered that the selectivity and sharpness of PDMS deposition on Au for inkless printing (i.e., negative) is significantly better than the traditional (positive) microcontact printing where the stamp is "inked" with low molecular weight PDMS.

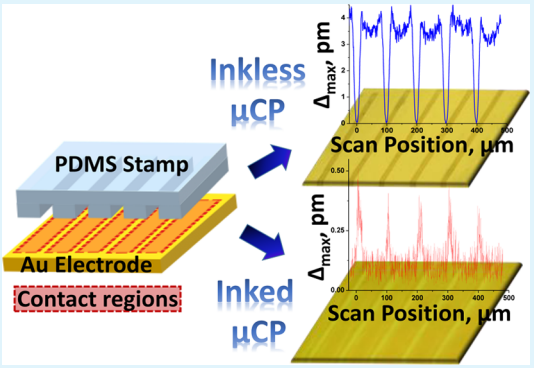

KEYWORDS: *soft lithography, surface diffusion, inkless printing, microcontact printing, negative printing, electrochemical passivation*

INTRODUCTION

Microcontact printing (μCP), or soft lithography, developed during the early 1990s for the patterning of self-assembled monolayers (SAMs) onto substrates, is a well-established method for generating microscale to nanoscale patterns with high versatility and accuracy.[1] Following the emergence of this technique, a wide range of applications using μCP, including tissue engineering,[2] electronic nanodevices,[3−5] and cell cocultures,[6,7] have been reported. In μCP, the relief features of a patterned elastomeric stamp, typically made up of polydimethylsiloxane (PDMS), are "inked" with molecules and then brought into contact with a substrate.[8] However, a growing number of studies over the past decade have reported that a significant amount of low-molecular-weight PDMS fragments transfer along with the ink during the μCP process.[9−13] Despite the fact that PDMS contamination during μCP is a deleterious side effect that can compromise the integrity of the printed samples, there are positive impacts, such as improving DNA adsorption on the PDMS stamp[13] and protein absorption on hydrophobic antibodies.[14] In addition, this PDMS "contamination" has also been developed into a new patterning technique called "inkless" microcontact printing (IμCP).[15]

In IμCP, the low molecular weight PDMS oligomers that spontaneously diffuse to the surface to lower the surface energy of the stamp[16,17] naturally transfer to the substrate on contact. Subsequent modification of the stamped feature may be performed by either leveraging the large surface energy (i.e., wettability) contrast[15] or functionalizing the deposited PDMS for selective deposition for device fabrication.[18,19] The IμCP method has been used to make devices such as organic semiconductor thin film transistors,[20] single-electron devices,[3,18,19] and biomolecular chips.[13,14,21]

Here, a nonintuitive feature of IμCP is described where PDMS from the stamp was transferred onto a Au surface that was not in contact with the stamp, while no polymer was transferred from the stamp where it contacted the Au surface. While on a silica surface, similar to standard IμCP, transfer of PDMS occurred at the contact region. The soft-lithography patterning was characterized by three methods that complement each other: (1) atomic force microscopy (AFM), used to measure the relative thickness of PDMS deposition between contact and noncontact regions; (2) Scanning Electrometer for Electrical Double-Layer (SEED),[22] a novel electrochemical method that measured the local passivation of the Au electrode at submonolayer sensitivity; and (3) field-emission scanning electron microscopy (FESEM), used to image a nanoparticle necklace[3,18,19] selectively deposited on the PDMS, to characterize the submonolayer transfer of polymer onto Au and silica during stamping. For both Au and silica substrates, the PDMS

Received: June 6, 2014
Accepted: August 6, 2014
Published: August 6, 2014

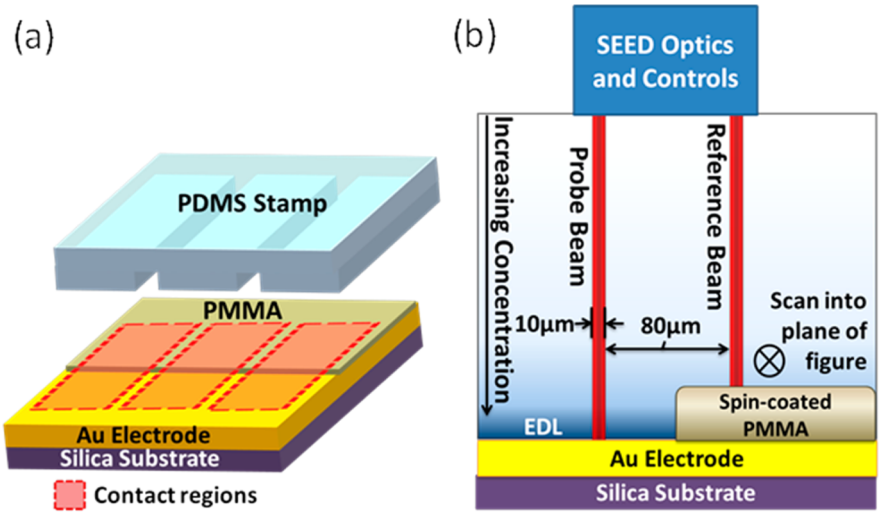

Figure 1. Experimental setup for SEED measurement. (a) The PDMS stamp is 80 μm wide lines spaced by 20 μm grooves. The contact pattern was orthogonal to a passivating PMMA layer interface. (b) SEED measured the electrochemical activity of the Au electrode by scanning along the PMMA line with the probe beam on the sample and the reference beam on the passivated PMMA layer.

pattern transferred onto the surface was also indirectly confirmed by optical microscopy. The observation was analyzed to explain the anomalous PDMS transfer morphology onto Au in contrast to a silica surface.

EXPERIMENTAL METHODS

Soft Lithography. *A. SU-8 Mold Fabrication.* The mold was fabricated with negative photoresist SU-8, which was diluted by mixing SU-8 developer in a 1:1 ratio. The diluted SU-8 was pipetted onto a 1 in. diameter silicon wafer and spin-coated at 3000 rpm for 30 s. The SU-8-coated wafer was heated at 60 °C for 30 s and then 120 °C for 1 min. The resist was exposed to 300 W of UV light for 2 min with a mask of 80 μm wide lines at 20 μm pitch. The resist was then developed to form a mold of a periodic pattern of 20 μm grooves with 80 μm spacing. The thickness of SU8, as measured by alpha-step, was 3 μm. The same procedure was repeated for another mask with a reverse pattern. The resulting mold had an alternating pattern of 80 μm lines with 20 μm spacing.

B. PDMS Stamp Preparation. The stamps for both μCP and IμCP were fabricated in a 10:1 ratio of PDMS and a cross-linking agent using PDMS (Sylgard 184) purchased from Dow Corning. The PDMS mixture was thoroughly mixed and degassed under vacuum for 10 min. The solution was poured into a 60 mm diameter Petri dish containing the SU-8 mold. The PDMS was cured at 60 °C for 30 min (IμCP) or 24 h (μCP) and released from the mold to form a PDMS stamp.

C. Stamping Process. The substrate to be stamped was a Si chip passivated with a 500 nm thick thermal oxide layer of silica. A layer of six 50 nm thick Au electrodes was deposited on a SiO_2/Si chip using a 10 nm thick TiO_2 adhesion layer by standard lithography. The chips were treated in piranha solution (1:3 volume ratio of 50 wt % H_2O_2 and 95.0−98.0% H_2SO_4) to make the surface hydrophilic. For IμCP, the cured stamp was placed directly onto the piranha-treated chip at 60 °C for 5 min. For μCP, the stamp was deposited on a thin film of "ink" prior to transferring the pattern. The ink was prepared by mixing a 1:1 ratio of PDMS (viscosity 1500 cSt) and a cross-linking agent (Gelest Inc.) followed by a 25 times dilution with hexane. The solution was spin-coated at 3000 rpm for 30 s on a coverslip. The PDMS stamp was placed onto the coverslip immediately after spin-coating. The assembly was heated at 60 °C for 3 min to partially cure the "ink". The inked stamp was immediately placed on the chip for 5 min to transfer the pattern.

D. High Resolution Printing. For printing a 5 μm feature, the mold was etched in a Si chip. A Si(100) wafer was coated with Shipley S1813 photoresist. A pattern on the resist was "written" using a Heidelberg DWL66 Laser Writer with a 40 mW solid state diode laser source at a wavelength of 405 nm. The resist was then developed to form a periodic pattern of 5 μm grooves with 80 μm spacing. Using reactive ion etching, the exposed Si wafer was subsequently etched by SF_6 (200 W; 50 mTorr) at an etching rate of 3000 Å/min for 10 min to form 5 μm wide trenches at interline spacing of 80 μm. The subsequent processes employed to make the PDMS stamp using the Si mold and IμCP were similar to those described in sections B and C above.

Characterization of PDMS Deposition. *A. SEED Measurement on Au.* A home-built instrument called Scanning Electrometer for Electrical Double-Layer (SEED) was developed to quantitatively measure the local electrochemical activity at the site of incidence of the sample laser beam (Figure 1).[22] The electrochemical redox reaction was regulated by a standard three-electrode potentiostat (Princeton Applied Research 273A). The Au electrode was the working electrode, the reference electrode was a homemade Ag/AgCl electrode, and the Pt-coated wall of the electrochemical chamber was the counter electrode. An AC potential of 200 mV amplitude at 2 kHz was applied to the Au electrode. The AC potential oscillated the ion concentration in the electrical double layer (EDL) to cause a modulation in the optical path length, typically by a few picometers. Due to charge compensation by the EDL, the ion oscillation in 100 mM solutions is restricted to ~20 nm, that is, about 10 times the Debye length.[23] SEED is a differential interferometer that measures the amplitude of the path length modulation (Δ) due to the applied AC potential[22,23] on the Au electrode as a function of potential difference between it and the solution. The potential of the solution was controlled by a reference electrode, Ag/AgCl. The Δ was measured interference between the probe beam and the reference beam (Figure 1b). The reference beam was incident on the Au electrode passivated by spin-coating 300 nm thick poly(methyl methacrylate) (PMMA). The spot size of the laser beam was 10 μm in diameter.[24] Because of the close proximity between the optical paths of the two beams, thermal noise was greatly reduced to yield a robust signal (i.e., Δ) with picometer sensitivity. When the electrode relative to the solution was at the potential of zero charge (PZC),[25] the EDL was least charged leading to the deepest penetration of the AC electric field into the solution resulting in maximum ion oscillation, Δ_{max}. This potential was found via a DC sweep. The samples were then scanned with a DC bias of this potential added to the AC probe signal.

B. AFM Scanning on Au and Silica. A Bruker Dimension Icon atomic force microscope was used to characterize the PDMS transfer onto the surface of both Au and silica. The scanning was performed by a ScanAsyst program with automatic image optimization technology.

C. Visualization of Nanoparticle Necklace on Au and Silica. The deposition of PDMS was visualized by depositing a monolayer of Au

nanoparticle necklaces that selectively deposited on the PDMS-coated surface. The necklace synthesis was described previously.[26,27] Briefly, a 10 mM HCl solution was added dropwise to 1 mL of a 10 nm diameter Au nanoparticle suspension at pH ~ 7 with 5.7×10^{12} particles/mL (BBI International) to form nanoparticle necklaces. The formation of these necklaces was evidenced by a change in color from wine-red to violet-blue in 12 h due to the shift in the surface plasmon resonance (SPR) absorption band from 525 to 610 nm in the UV–vis spectrum.[27,28] The necklace suspension was stable for well over 5 days.

After IμCP, the sample was treated with ammonia plasma (70 W; 465 mTorr; 60 s) to positively charge the transferred PDMS. The sample was immediately immersed in the Au nanoparticle necklace solution for ~16 h to deposit the negatively charged necklaces. The necklace deposited was imaged by using a Hitachi S4700 field-emission scanning electron microscope. Studies have shown that the necklace array exclusively deposits on the PDMS surface that was functionalized by ammonia plasma, and a single monolayer of PDMS is sufficient to initiate deposition.[18,19]

RESULTS AND DISCUSSION

For a PDMS stamp with a feature of 80 μm wide lines spaced by 20 μm, the resulting patterns on the sample following IμCP are shown in Figure 2. The optical image clearly demonstrated a contrast between the contact and noncontact regions on both the Au and silica surfaces. A region with slightly "burred" edges was chosen to demonstrate that, on Au, it appears that the PDMS deposition is on the noncontact region. The slightly peeled edges may have occurred when the stamp was lifted off. The contrast on silica was also observed, but the nature of the transfer was not apparent. To quantify the material transfer on IμCP, the features were analyzed by the analytical methods mentioned in the Experimental Methods section. The stamping characteristics on Au are addressed first followed by silica.

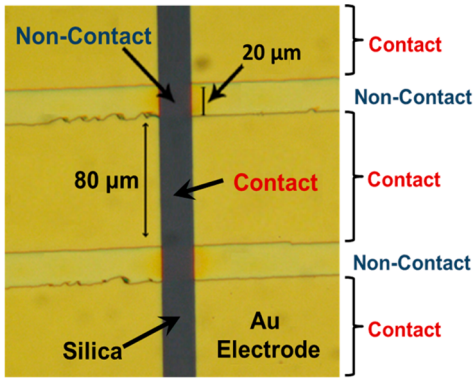

Figure 2. Optical image of IμCP pattern. The difference in coloration indicates a clear contrast between the contact and noncontact regions.

PDMS Transfer on Au: Negative Printing. The AFM image showed a PDMS deposition on the noncontact region with a width of ~18 μm and a thickness of 15 nm (Figure 3a). The width being slightly smaller than the 20 μm groove was attributed to the deformation of the PDMS features caused by the pressure applied during the stamping process. A sharp increase in height at the edges was observed. The enhancement in deposition at the edges was attributed to stress concentration at the edges, that is, the "hole-punch" effect.[29] To evaluate the absolute thickness on the two surfaces, the level of passivation on the contact regions was evaluated by SEED (Figure 1). As the laser beams were scanned along the PMMA/patterned Au electrode interface, repeating patterns of 20 μm passivation spaced by 80 μm were observed. The low Δ_{max} that was observed over the 20 μm (noncontact) regions indicated that the noncontact regions were, as expected, passivated with PDMS (Figure 4). A high Δ_{max} observed on the 80 μm (contact) regions was similar to a pristine Au electrode (Figure S1 in the Supporting Information), indicating that virtually no PDMS transfer occurred on the contact regions. (Just a monolayer of three carbon surfactant ($HS-CH_2CH_2CH_3$) is sufficient to passivate the surface.) The comparison between the SEED signal and the optical image showed that the minimum Δ_{max} was consistent with the PDMS lines having printed on the noncontact regions. Thus, the 15 nm transfer in the noncontact regions was the absolute thickness of PDMS on stamping. To eliminate the possibility of the size effects due to the feature width of the stamp, a stamp with a reversed feature (i.e., 20 μm lines spaced at 80 μm) was studied. The AFM

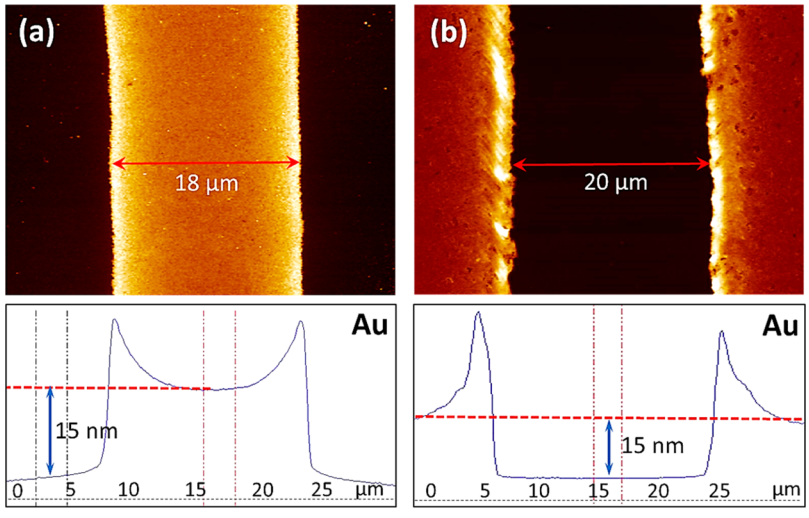

Figure 3. AFM scanning on Au surface. (a) Using a stamp with a feature of 80 μm wide lines spaced by 20 μm, PDMS deposited on the noncontact region with a width of ~18 μm and a thickness of 15 nm. (b) Reversing the feature size of the stamp, deposition of PDMS with a thickness of 15 nm is observed on the 80 μm noncontact regions. Considering the similar stamping behavior in both respects, the results indicated a negative printing effect of IμCP on a Au substrate.

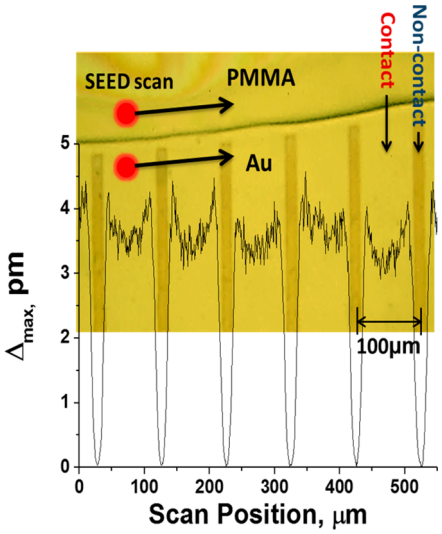

Figure 4. Line scan by SEED with optical microscope image. As the two laser beams (shown schematically) were scanned over the pattern, the Δ_{max} modulated consistent with the pattern. The PDMS deposition region corresponding to passivation indicative of minimum Δ_{max} was consistent with the width of the noncontact region.

analysis indicated that the IμCP exhibited similar behavior (Figure 3b). The deposition of polymer took place exclusively on the 80 μm noncontact regions with the same thickness of ~15 nm and the enhancement at the edges.

Next, we consider the mechanism for explaining the anomalous observation of IμCP stamping behavior on the Au surface. We assumed that the adhesion of PDMS to Au was poor and thus the (uncross-linked) low molecular weight PDMS in the stamp did not transfer on contact. The low molecular weight PDMS that was expected to leach out at the interface consists of eight units of cyclic (unreacted) monomers and their higher homologue.[30] In contrast, for the inked stamp, where there was excess PDMS on the surface, conventional transfer of polymer on the contact region on Au did occur (see the Supporting Information, Figure S2). However, the low molecular weight PDMS also coated on the "open surface" (not in contact with the stamp) by surface diffusion,[31,32] driven by the low surface energy of the polymer relative to Au.[10,15,33] As a result, the relative thickness contrast of PDMS was small. Using SEED, the contrast between the contact and the contact region for μCP (i.e., inked) and IμCP (inkless) was 2 versus 74, indicating the latter is a better mode of printing on Au (Figure S3 in the Supporting Information).

Surface diffusion occurs via a precursor film of PDMS, which is a nanometer thin film at the spreading front.[11,34−36] To verify the surface diffusion mechanism, we examined the effect of the stamping temperature on IμCP. Consistent with the (exponential) increase in diffusion coefficient with temperature, the thickness of the PDMS in the noncontact region increased significantly as the stamping temperature increased (Figure 5). The precursor layer spread relatively quickly, typically at a velocity of ~30 μm/min at 25 °C for high molecular weight PDMS.[32] It has also been demonstrated that the rate was higher initially[37] and increased with lower molecular weight PDMS,[38] as well as with improved surface interaction.[39,40] As a result, for 20−80 μm gaps at 60 °C, the spreading was too fast to freeze the precursor layer at a reasonably different penetration depth. For all of the three conditions, on the contact regions, no residue of low molecular weight PDMS was transferred due to the poor adhesion of the polymer with the Au surface (as determined by SEED) (i.e., the Au/PDMS contact was "clean"). Furthermore, because the noncontact area was flanked by the two PDMS edges that were the source of the polymer, the enhancement of the thickness at the edges was expected with a minimum in the middle (Figure 5). Thus, apart from the "punch-hole effect" noted above, the surface diffusion profile also contributed to the enhancement at the edges.

To further corroborate the above observation, nanoparticle necklaces were deposited as a marker to probe the deposition of PDMS (see Experimental Methods section for details) (Figure 6). Consistent with SEED observation (Figure 4) and the mechanism discussed above, SEM images clearly show deposition of necklaces on the Au surface which was not in contact during stamping (Figure 6c). However, for the silica surface, the PDMS was deposited exclusively on the contact region. In other words, the surface diffusion of PDMS on silica was negligible. This "checkerboard" deposition of PDMS by

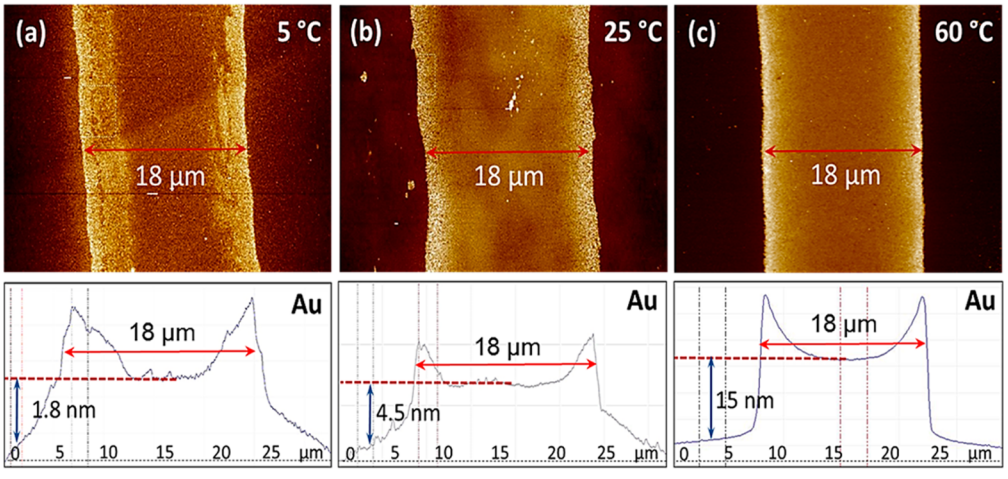

Figure 5. AFM scanning of PDMS on Au surface printed at different temperatures. (a) At 5 °C, the rate of surface diffusion was the lowest, leading to deposition of the thinnest PDMS layer (~1.8 nm) on the Au surface. (b) Elevating the temperature to room temperature increased the rate of diffusion, PDMS layer deposited was relatively thicker (~4.5 nm). (c) At a temperature of 60 °C, deposition of PDMS was the thickest (~15 nm) due to the greatest rate of surface diffusion by high mobility of polymer.

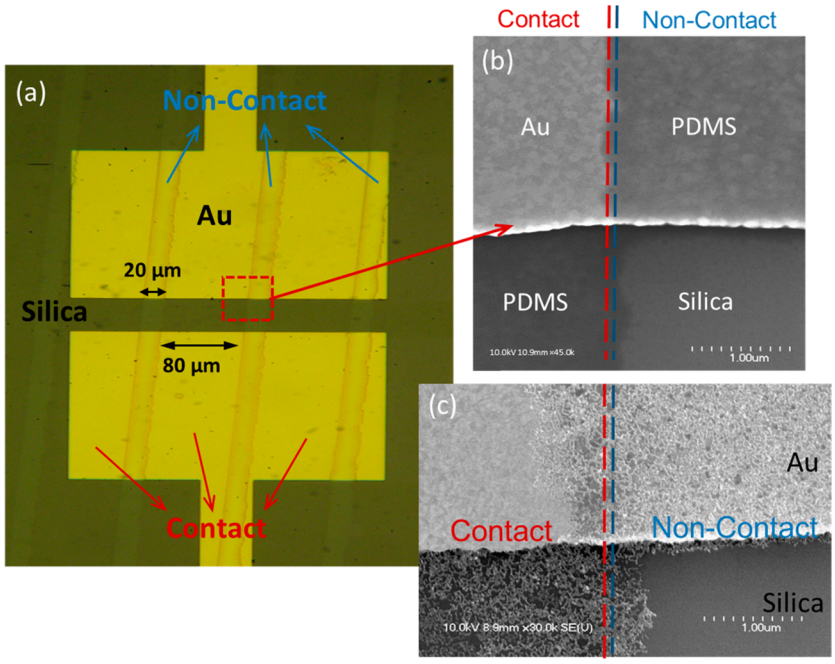

Figure 6. Optical and FESEM images of checkerboard patterning. (a) Optical image of IμCP. (b) SEM image showed the opposite PDMS transfer effect on Au and silica substrates. (c) Au nanoparticle necklace deposition further demonstrated the opposite effects of IμCP on Au and silica substrates.

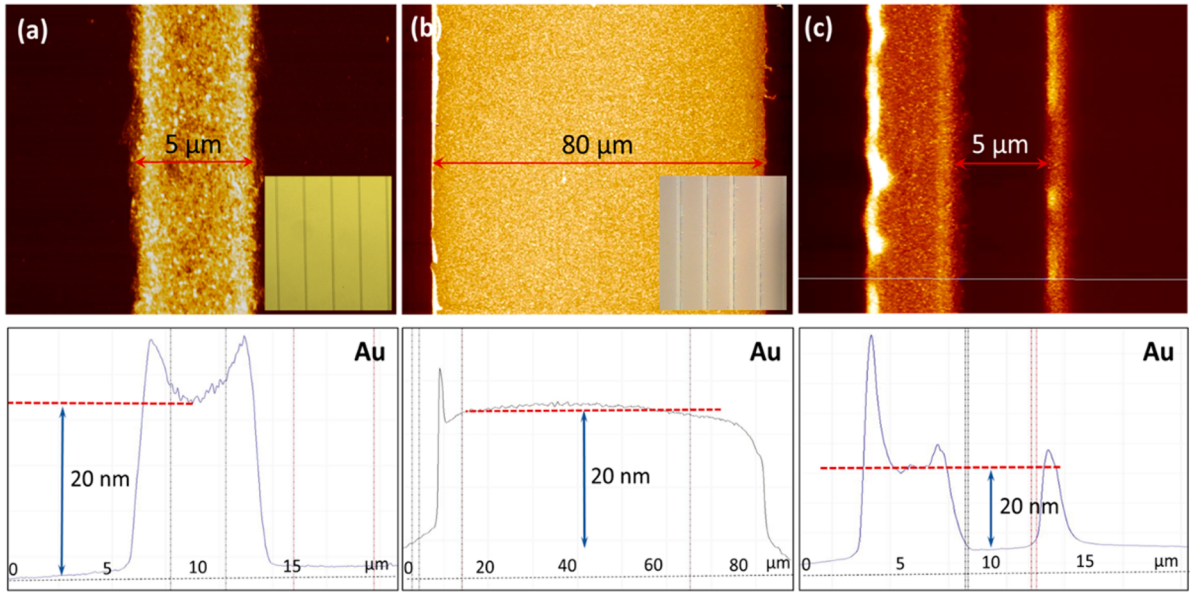

Figure 7. AFM scanning of high resolution PDMS on Au surface. (a) Using a PDMS stamp of 80 μm lines spaced by 5 μm, PDMS deposited on the 5 μm noncontact region of Au with a thickness of 20 nm. Inset: Optical image of PDMS pattern. (b) Reversing the stamp features, PDMS layer deposited uniformly onto the entire 80 μm noncontact region. Inset: Optical image of PDMS pattern. (c) Upon placing a weight of 100 g on the PDMS stamp while printing, the "roof collapse" effect occurred due to stamp instability.

contact and noncontact on the Au/silica interface is further considered in the next subsection by analyzing the stamping on the silica surface.

High Resolution Negative Printing. Using the Si mold described in the Experimental Methods section, PDMS was patterned on a Au substrate by IμCP at conditions similar to Figure 3. The optical images of 5 μm lines on 80 μm pitch and 80 μm lines on 5 μm pitch showed reasonably high-quality printing on a large area (Figure 7 inset). The AFM scan, similar to Figure 3, showed negative printing on Au, as expected (Figure 7a and b). Remarkably, the deposition on the 80 μm wide noncontact region between the 5 μm wide ridges was fairly uniform (Figure 7b) indicating that even if there was sagging, the surface diffusion was not hindered. To exaggerate the sagging effect in the unsupported 80 μm wide span, 100 g of dead weight was placed over an area of 4.9 cm^2. The result was nonuniform deposition (Figure 7c). As expected, the 5 μm region in Figure 7c in contact with the substrate had no PDMS deposition. However, the 80 μm region that should have uniform PDMS deposition (similar to Figure 7b) also had

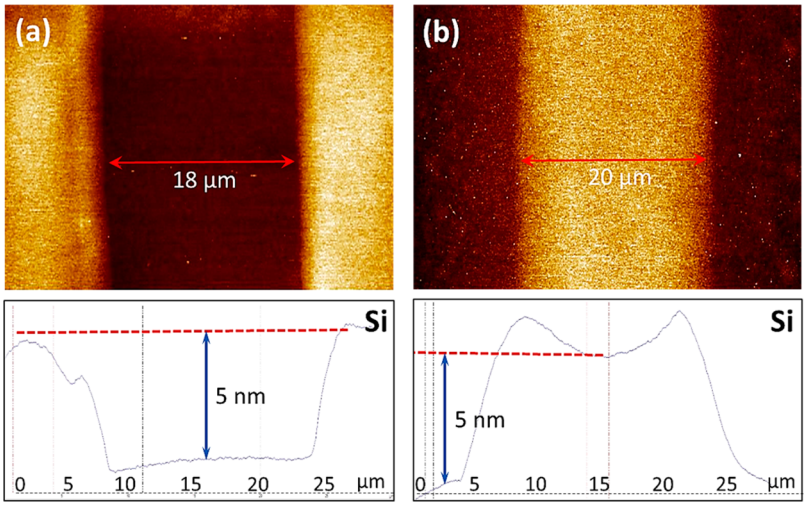

Figure 8. AFM scanning on silica substrates patterned by IμCP in Figure 3. (a) 5 nm thick low molecular weight PDMS deposited on the regions in contact with the stamp, generated a "clean" channel with a width of ~18 μm. (b) Reversing the feature size of the stamp, deposition of PDMS was observed on the 20 μm contact regions. The size of the width in Figure 6a and b is consistent with that in Figure 3a and b, respectively.

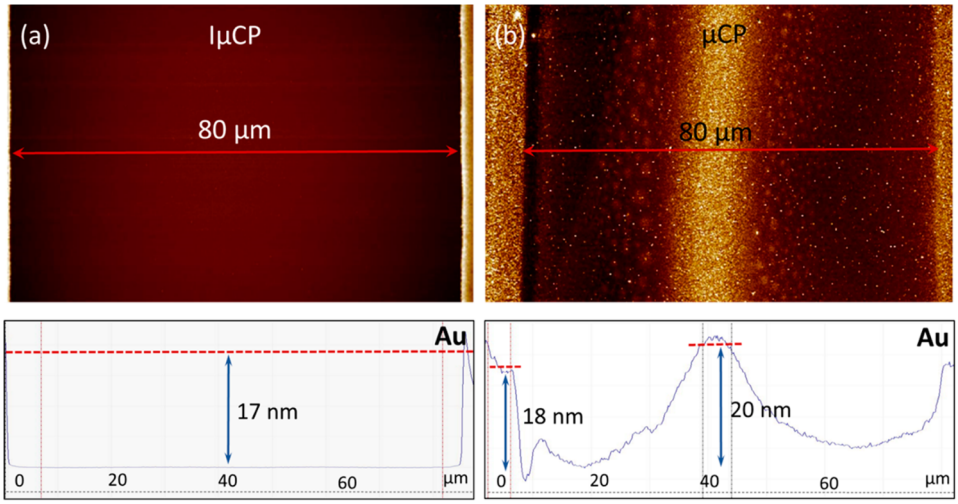

Figure 9. AFM scanning on Au with small features by large spacing patterned by IμCP and μCP. (a) IμCP resulted in a "clean" 80 μm region (contact region) flanked by 5 μm PDMS features on each side. (b) μCP showed 5 μm PDMS features on each side with a nonuniform printing of PDMS across the 80 μm region due to "roof collapse", a result of poor mechanical support.

regions where there was no PDMS deposition. These "blackout" regions in the 80 μm wide gap were attributed to "roof collapse" where the unsupported PDMS mold, due to its weight, contacted the surface to prevent surface diffusion.

PDMS Transfer on Silica: Positive Printing. Next we discuss IμCP where the effect on the silica substrate is more conventional (i.e., the PDMS deposits on the contact region (Figure 6)). As the nanoparticle necklace deposition is sensitive to a submonolayer of PDMS,[19] no deposition on the noncontact region indicated that the deposition on the contact region was exclusive. Using AFM for the stamp with 18 and 80 μm wide lines (same as Figure 3), the PDMS deposition on the contact regions was ~5 nm (Figure 8). As no deposition occurred on the noncontact region (Figure 6), the PDMS thickness of 5 nm was absolute. The small "wrinkles" in thickness at the interface were attributed to the distortion of the PDMS edge as a result of pressure. The conventional (expected) positive printing suggested that the adhesive interaction of PDMS with silica was strong, and the surface diffusion influenced deposition on the noncotact region was negligible.

The strong adhesion of PDMS to silica is attributed to a specific interaction of PDMS with the hydroxylated surface, which was formed by exposing the silica to piranha.[41] As a result, a thin PDMS film was deposited upon peeling off the PDMS stamp from the silica surface. The (complete) depletion of PDMS on silica (Figure 6) was surprising but may be attributed to evaporation. The vapor pressure of low-weight PDMS oligomers was reasonably high for significant evaporation at 60 °C.[42] On the noncontact regions, similar to the Au surface, an ultrathin low molecular weight PDMS precursor film should be transferred onto the silica by surface diffusion. However, the thickness of the precursor film on silica should be much smaller than on Au owing to the higher polarizability of the latter.[34,39] As a result of evaporation, the thin layer of PDMS evaporated entirely from the silica surface. Evaporation occurred on Au as well, but the PDMS film was thick enough for a substantial amount of material to be left over after evaporation.

Comparison Between μCP and IμCP. Potential application of negative printing on Au stems from two key characteristics of the process. (i) The deposition for IμCP had an order of magnitude higher contrast compared to μCP (Figure S3 in the Supporting Information). Importantly, for IμCP, the noncontact area was completely passivated while the contact area was clean, comparable to pristine Au (see Figures 3, 4, 7, and 9a). The lower contrast in μCP arose because both surface diffusion (in the noncontact region) and ink transfer (in the contact region) occurred. (ii) For printing small features with large spacing, for instance, 5 μm spaced by 80 μm, IμCP is more reliable than (conventional) μCP. In the latter, the features may distort because of "roof collapse" (Figure 9), while in the former the larger regions are in contact with the surface to provide mechanical support. The high contrast and small features with large pitch are potentially an additional method in the tool box for making larger area devices by soft lithography on flexible substrates, as indicated in the Introduction.[3,13,14,18−21]

CONCLUSIONS

Inkless microcontact printing (IμCP) was studied on Au and silica surfaces. The resulting pattern was an interplay of interfacial adhesion, surface diffusion, and evaporation. It was discovered that the uncured, low molecular weight PDMS was exclusively transferred onto the noncontact region for Au (i.e., negative printing) while the complete opposite occurred for silica (i.e., positive printing). The anomalous negative printing on Au was explained by surface diffusion. An opto-electrochemical method called SEED revealed that the PDMS deposition was exclusively on the noncontact region while the Au in contact with the stamp remained pristine. The submonolayer deposition of PDMS was further imaged by Au nanoparticle necklaces that exclusively deposited on a polymer modified surface. The SEM image of the necklace revealed perfect positive printing on silica, while no necklace deposition occurred on the noncontact region. The SEM image was consistent with perfect negative printing as measured by SEED on Au. As a result, the positive and negative printing at the Au/silica interface was termed a "checkerboard" structure. From the AFM scan, the edges of PDMS transfer were significantly sharper for negative printing. An interesting application of IμCP phenomenon on Au is achieving small features: the softness of PDMS limits the sharpness of printing due to mechanical deformation of the stamp.[43] The problem could be averted by IμCP where the image is "negative" where the small feature is the groove rather than the highly deformable protrusion.

ASSOCIATED CONTENT

Supporting Information

Stamping process for microcontact printing (μCP), microcontact printing with ink, and comparison of scans of different curing schemes. This material is available free of charge via the Internet at http://pubs.acs.org/.

AUTHOR INFORMATION

Corresponding Author

*E-mail: rsaraf2@unl.edu.

Notes

The authors declare no competing financial interest.

ACKNOWLEDGMENTS

R.F.S. would like to thank the NSF (CBET-1353125) for financial support.

REFERENCES

(1) Xia, Y. N.; Whitesides, G. M. Soft Lithography. *Annu. Rev. Mater. Sci.* **1998**, *28*, 153−184.
(2) Kane, R. S.; Takayama, S.; Ostuni, E.; Ingber, D. E.; Whitesides, G. M. Patterning Proteins and Cells Using Soft Lithography. *Biomaterials* **1999**, *20*, 2363−2376.
(3) Kane, J.; Ong, J.; Saraf, R. F. Chemistry, Physics, and Engineering of Electrically Percolating Arrays of Nanoparticles: A Mini Review. *J. Mater. Chem.* **2011**, *21*, 16846−16858.
(4) Rogers, J. A.; Bao, Z.; Baldwin, K.; Dodabalapur, A.; Crone, B.; Raju, V. R.; Kuck, V.; Katz, H.; Amundson, K.; Ewing, J.; Drzaic, P. Paper-Like Electronic Displays: Large-Area Rubber-Stamped Plastic Sheets of Electronics and Microencapsulated Electrophoretic Inks. *Proc. Natl. Acad. Sci. U.S.A.* **2001**, *98*, 4835−4840.
(5) Roman, L. S.; Inganas, O.; Granlund, T.; Nyberg, T.; Svensson, M.; Andersson, M. R.; Hummelen, J. C. Trapping Light in Polymer Photodiodes with Soft Embossed Gratings. *Adv. Mater.* **2000**, *12*, 189−195.
(6) Folch, A.; Toner, M. Microengineering of Cellular Interactions. *Annu. Rev. Biomed. Eng.* **2000**, *2*, 227−256.
(7) Whitesides, G. M.; Ostuni, E.; Takayama, S.; Jiang, X.; Ingber, D. E. Soft Lithography in Biology and Biochemistry. *Annu. Rev. Biomed. Eng.* **2001**, *3*, 335−373.
(8) Kumar, A.; Whitesides, G. M. Features of Gold Having Micrometer to Centimeter Dimensions can be Formed through a Combination of Stamping with an Elastomeric Stamp and an Alkanethiol "Ink" Followed by Chemical Etching. *Appl. Phys. Lett.* **1993**, *63*, 2002−2004.
(9) Bohm, I.; Lampert, A.; Buck, M.; Eisert, F.; Grunze, M. A Spectroscopic Study of Thiol Layers Prepared by Contact Printing. *Appl. Surf. Sci.* **1999**, *141*, 237−243.
(10) Graham, D. J.; Price, D. D.; Ratner, B. D. Solution Assembled and Microcontact Printed Monolayers of Dodecanethiol on Gold: A Multivariate Exploration of Chemistry and Contamination. *Langmuir* **2002**, *18*, 1518−1527.
(11) Glasmastar, K.; Gold, J.; Andersson, A. S.; Sutherland, D. S.; Kasemo, B. Silicone Transfer During Microcontact Printing. *Langmuir* **2003**, *19*, 5475−5483.
(12) Kim, J. H.; Hwang, H. S.; Hahm, S. W.; Khang, D. Y. Hydrophobically Recovered and Contact Printed Siloxane Oligomers for General-Purpose Surface Patterning. *Langmuir* **2010**, *26*, 13015−13019.
(13) Thibault, C.; Severac, C.; Mingotaud, A.; Vieu, C.; Mauzac, M. Poly(dimethylsiloxane) Contamination in Microcontact Printing and Influence on Patterning Oligonucleotides. *Langmuir* **2007**, *23*, 10706−10714.
(14) Wigenius, J. A.; Fransson, S.; Post, F.; Inganas, O. Protein Biochips Patterned by Microcontact Printing or by Adsorption-Soft Lithography in Two Modes. *Biointerphases* **2008**, *3*, 75−82.
(15) Wang, X. J.; Ostblom, M.; Johansson, T.; Inganas, O. PEDOT Surface Energy Pattern Controls Fluorescent Polymer Deposition by Dewetting. *Thin Solid Films* **2004**, *449*, 125−132.
(16) Fox, T. G.; Flory, P. J. The Glass Temperature and Related Properties of Polystyrene. Influence of Molecular Weight. *J. Polym. Sci.* **1954**, *14*, 315−319.
(17) Zhao, W.; Zhao, X.; Rafailovich, M. H.; Sokolov, J.; Composto, R. J.; Smith, S. D.; Satkowski, M.; Russell, T. P.; Dozier, W. D.; Mansfield, T. Segregation of Chain Ends to Polymer Melt Surfaces and Interfaces. *Macromolecules* **1993**, *26*, 561−562.
(18) Yu, C.; Lee, S.-W.; Ong, J.; Moore, D.; Saraf, R. F. Single Electron Transistor in Aqueous Media. *Adv. Mater.* **2013**, *25*, 3079−3084.
(19) Ong, J. K. Y.; Nguyen, C. V.; Sayood, S.; Saraf, R. F. Imaging Electroluminescence from Individual Nanoparticles in an Array

Exhibiting Room Temperature Single Electron Effect. *ACS Nano* **2013**, *7*, 7403−7410.
(20) Briseno, A. L.; Roberts, M.; Ling, M. M.; Moon, H.; Nemanick, E. J.; Bao, Z. N. Patterning Organic Semiconductors Using "Dry" Poly(dimethylsiloxane) Elastomeric Stamps for Thin Film Transistors. *J. Am. Chem. Soc.* **2006**, *128*, 3880−3881.
(21) Asberg, P.; Nilsson, K. P. R.; Inganas, O. Surface Energy Modified Chips for Detection of Conformational States and Enzymatic Activity in Biomolecules. *Langmuir* **2006**, *22*, 2205−2211.
(22) Singh, G.; Saraf, R. F. Direct Measurement of Ion Accumulation at the Electrode Electrolyte Interface under an Oscillatory Electric Field. *J. Phys. Chem. B* **2006**, *110*, 12581−12587.
(23) Lee, S.-W.; Lopez, J.; Saraf, R. F. Direct Mapping of Local Redox Current Density on a Monolith Electrode by Laser Scanning. *Biosens. Bioelectron.* **2013**, *47*, 408−414.
(24) Singh, G.; Moore, D.; Saraf, R. F. Localized Electrochemistry on a 10 μm Spot on a Monolith Large Electrode: An Avenue for Electrochemical Microarray Analysis. *Anal. Chem.* **2009**, *81*, 6055−6060.
(25) Bode, D. D.; Andersen, T. N.; Eyring, H. Anion and pH Effects on the Potentials of Zero Charge of Gold and Silver Electrodes. *J. Phys. Chem.* **1967**, *71*, 792−797.
(26) Kane, J.; Inan, M.; Saraf, R. F. Self-Assembled Nanoparticle Necklaces Network Showing Single-Electron Switching at Room Temperature and Biogating Current by Living Microorganisms. *ACS Nano* **2010**, *4*, 317−323.
(27) Maheshwari, V.; Kane, J.; Saraf, R. F. Self-Assembly of a Micrometers-Long One-Dimensional Network of Cemented Au Nanoparticles. *Adv. Mater.* **2008**, *20*, 284−287.
(28) Lin, S.; Li, M.; Dujardin, E.; Girard, C.; Mann, S. One-Dimensional Plasmon Coupling by Facile Self-Assembly of Gold Nanoparticles into Branched Chain Networks. *Adv. Mater.* **2005**, *17*, 2553−2559.
(29) Johnson, K. L. *Contact Mechanics*, 1st ed.; Cambridge University Press: Cambridge, 1985.
(30) Lee, J. N.; Park, C.; Whitesides, G. M. Solvent Compatibility of Poly(dimethylsiloxane)-Based Microfluidic Devices. *Anal. Chem.* **2003**, *75*, 6544−6554.
(31) Voue, M.; Valignat, M. P.; Oshanin, G.; Cazabat, A. M.; De Coninck, J. Dynamics of Spreading of Liquid Microdroplets on Substrates of Increasing Surface Energies. *Langmuir* **1998**, *14*, 5951−5958.
(32) Zbik, M. S.; Frost, R. L. PDMS Spreading Morphological Patterns on Substrates of Different Hydrophilicity in Air Vacuum and Water. *J. Colloid Interface Sci.* **2010**, *344*, 563−574.
(33) Cortese, B.; Piliego, C.; Viola, I.; D'Amone, S.; Cingolani, R.; Gigli, G. Engineering Transfer of Micro- and Nanometer-Scale Features by Surface Energy Modification. *Langmuir* **2009**, *25*, 7025−7031.
(34) de Gennes, P. G. Wetting: Statics and Dynamics. *Rev. Mod. Phys.* **1985**, *57*, 827−863.
(35) Heslot, F.; Fraysse, N.; Cazabat, A. M. Molecular Layering in the Spreading of Wetting Liquid Drops. *Nature* **1989**, *338*, 640−642.
(36) Marmur, A. Equilibrium and Spreading of Liquids on Solid Interfaces. *Adv. Colloid Interface Sci.* **1983**, *19*, 75−102.
(37) Valignat, M. P.; Fraysse, N.; Cazabat, A. M.; Heslot, F. Molecular Networks in the Spreading of Microdroplets. *Langmuir* **1993**, *9*, 601−603.
(38) Silberzan, P.; Léger, L. Spreading of High Molecular Weight Polymer Melts on High-Energy Surfaces. *Macromolecules* **1992**, *25*, 1267−1271.
(39) Yang, L.; et al. Effect of Surface Free Energy on PDMS Transfer in Microcontact Printing and Its Application to ToF-SIMS to Probe Surface Energies. *Langmuir* **2009**, *25*, 5674−5683.
(40) Heslot, F.; Cazabat, A. M.; Levinson, P.; Fraysse, N. Experiments on Wetting on the Scale of Nanometers: Influence of the Surface Energy. *Phys. Rev. Lett.* **1990**, *65*, 599−602.
(41) Bruinsma, R. Slow Spreading of Polymer Melts. *Macromolecules* **1990**, *23*, 276−280.
(42) Lei, Y. D.; Wania, F.; Mathers, D. Temperature-Dependent Vapor Pressure of Selected Cyclic and Linear Polydimethylsiloxane Oligomers. *J. Chem. Eng. Data* **2010**, *55*, 5868−5873.
(43) Perl, A.; Reinhoudt, D. N.; Huskens, J. Microcontact Printing: Limitations and Achievements. *Adv. Mater.* **2009**, *21*, 2257−2268.